



# Evaluation of bond stress-slip models for FRP reinforcing bars in concrete



Xiaoshan Lin, Y.X. Zhang\*

School of Engineering and Information Technology, The University of New South Wales at the Australian Defence Force Academy, Northcott Drive, Canberra, ACT 2600, Australia

## ARTICLE INFO

### Article history:

Available online 1 August 2013

### Keywords:

Bond stress-slip model  
FRP reinforcing bar  
Concrete  
Finite element analysis  
Surface condition

## ABSTRACT

In this paper several currently available bond stress-slip models for steel and FRP reinforcing bars in concrete are firstly reviewed, and both merits and demerits of these models are discussed. The models which are promising to be used for describing the bond-slip behaviour of FRP reinforcing bars in numerical analysis are evaluated through finite element analysis of FRP-reinforced concrete beams with bond-slip effect taken into account. A newly developed composite beam element with bond-slip is employed for finite element analysis of a GFRP-reinforced concrete beam and a CFRP-reinforced concrete beam with the selected bond stress-slip models built in the finite element model. The suitability and capability of the bond stress-slip models informed from the finite element analyses are summarised and concluded. Finally, parametric study is carried out on the most appropriate bond stress-slip model to investigate the effect of different surface conditions of reinforcing bars on the structural behaviour.

© 2013 Elsevier Ltd. All rights reserved.

## 1. Introduction

In recent years, fibre reinforced polymer (FRP) has been widely used in reinforced concrete structures due to its superior material properties, such as high tensile strength, excellent electrochemical corrosion resistance and cost effective fabrication, over the traditional steel reinforcements. Despite the obvious advantages of FRPs, they are not without drawbacks, and one major disadvantage is the comparatively weaker bond strength of FRP reinforcing bars (rebars) in concrete compared with traditional steel rebars.

In fact, bond between concrete and the reinforcing bars plays an important role in stress transferring from the former to the latter, and debonding has become one of the thorny issues in analysis of reinforced concrete structures. Bond between FRP reinforcing bars and the surrounding concrete is complicated and various factors may influence the bond characteristics of FRP reinforcements to concrete. For example, geometry and surface conditions of FRP rebars, concrete compressive strength, confinement pressure, rebar diameter and the position in the cast and specimen, embedment length, temperature changes and environmental conditions [1] will all affect the bonding capability between FRP rebars and the concrete.

So far, numerous experimental studies have been conducted to investigate the bond strength of FRP rebars in concrete as well as the influences of parameters, such as fibre type, surface treatment, bar diameter and temperature, on the bond characteristics of FRP rebars [2–6]. However, very few studies have been carried out to

determine the bond stress-slip constitutive law for FRP rebars, which is essential to finite element analysis of FRP-reinforced concrete structures. Therefore, perfect bonding was assumed in most of the numerical studies of FRP-reinforced concrete structures [7–12], resulting in non-realistic and imprecise predictions of the structural behaviour. In order to obtain a more accurate structural analysis, the bond-slip behaviour of FRP rebars in concrete should be considered in the numerical model. However, only several FRP bond stress-slip models have been reported so far, and the suitability and capability of these models for numerical modelling of FRP-reinforced concrete structures have not been justified yet.

This paper aims to give a review of the currently available bond stress-slip models for FRP rebars in concrete, as well as some models for traditional steel rebars which may be suitable for numerical analysis of FRP-reinforced concrete structures. Then the appropriateness and capability of the most promising and often used bond stress-slip models are investigated for FRP rebars. The paper is structured as follows. A brief review and introduction of the currently available bond stress-slip models for FRP rebars in concrete is given in Section 2, and both their merits and demerits are discussed. A few bond stress-slip models for steel rebars in concrete are presented in Section 3. In Section 4, three bond stress-slip models, i.e. the Eligehausen, Popov and Bertero (BPE) Model [13], the BPE Modified Model [1], and the Cosenza, Manfredi and Realfonzo (CMR) Model [14], which have been often used and seem to be the promising FRP bond stress-slip models for numerical analysis, are discussed in more details, and their appropriateness and capability are evaluated via finite element analysis of FRP-reinforced concrete beams by implementing them in a newly developed finite element model [15]. In addition, the appropriateness of two bond stress-slip

\* Corresponding author. Tel./fax: +61 2 62688169.  
E-mail address: [y.zhang@adfa.edu.au](mailto:y.zhang@adfa.edu.au) (Y.X. Zhang).

models, which were proposed by Harajli et al. [16] and Haskett et al. [17] for steel rebars, for finite element analyses of FRP-reinforced concrete structures is also evaluated in Section 4. Section 5 presents a parametric study using the most suitable bond stress-slip model for FRP rebars, and the effect of different rebar surfaces on the structural behaviour is investigated. Conclusions are drawn in the final section.

## 2. Bond stress-slip models of FRP rebars in concrete

At present, several bond stress-slip models for FRP rebars in concrete have been proposed in literature. An analytical expression for a monotonic bond stress-slip curve, which describes the bond stress between FRP rebars and concrete, was proposed based on experimental data by Malvar [18]. A bond-slip constitutive law known as the BPE Model, which was developed by Eligehausen et al. [13] for deformed steel bars, has been the most well-known and commonly used model in analysis of traditional steel-reinforced concrete structures [19–23]. This model was applied to represent the local bond stress-slip relationship of FRP rebars by Rossetti et al. [24] and Cosenza et al. [14] through calibrating the parameters based on the experimental results. Later, based on the BPE Model, Cosenza et al. [1] developed the BPE Modified Model, which describes the bond stress-slip relationship for FRP rebars, with the effects of different FRP rebar surfaces taken into account. After that, the BPE Modified Model has been utilised in a number of studies on FRP-reinforced concrete structures [25–27]. The CMR Model was proposed to be used as an alternative to the BPE Model by Cosenza et al. [14], but it is only for the ascending branch of the bond stress-slip curve. In addition, Tighiouart et al. [5] also proposed a model for the ascending part of the bond stress-slip relationship based on experimental data and calibration of the parameters in the CMR Model.

In this section, these currently available bond stress-slip models for FRP rebars are introduced and reviewed, and their merits and drawbacks are discussed.

### 2.1. Malvar's Model

The bond stress-slip relationship of FRP rebars in concrete proposed by Malvar [18] based on the pullout test data is supposed to be the first FRP bond stress-slip model. FRP rebars with three different types of surfaces (deformed and indented surface, indented surface and deformed surface) were tested in his study, and the effects of confinement and indentation depth on the bond strength were investigated. The bond stress-slip curve was then derived in a two-step procedure. First, the peak bond stress  $\tau_1$  and slip  $s_1$  were defined as a function of confining axisymmetrical radial pressure  $\sigma_r$ , as shown in Eqs. (1) and (2). Second, the expression of the complete bond stress-slip curve was defined as  $\tau = \tau(s, \sigma_r)$  given by Eq. (3). In addition, seven empirical constants were required to determine the shape of the curve which describes the entire bond stress versus loaded-end slip response.

$$\tau_1/f_t = A + B(1 - e^{-C\sigma_r/f_t}) \quad (1)$$

$$s_1 = D + E\sigma_r \quad (2)$$

where  $f_t$  is concrete tensile strength;  $A, B, C, D$  and  $E$  are empirical constants for different bar types.

$$\tau = \tau_1 \frac{F\left(\frac{s}{s_1}\right) + (G-1)\left(\frac{s}{s_1}\right)^2}{1 + (F-2)\left(\frac{s}{s_1}\right) + G\left(\frac{s}{s_1}\right)^2} \quad (3)$$

where  $\tau_1$  is the peak bond stress and  $s_1$  the slip at the peak bond stress.  $F$  and  $G$  are the empirical constants for different bar types.

In Malvar's study [18], those empirical constants were only evaluated for FRP rebars composed of E-glass fibres with two types of rebar surface treatment, and the effects such as fibre type and rebar diameter were not considered. Also, the value of confining axisymmetrical radial pressure  $\sigma_r$  is hard to be determined when analysing structures under bending load. Furthermore, Malvar's Model was assessed as being less reliable for modelling the ascending branch of the bond stress-slip relation curve of FRP [1].

### 2.2. BPE Model

BPE Model was first proposed for deformed steel bars by Eligehausen et al. [13], and then applied to represent the local bond stress-slip relationship of FRP rebars by Rossetti et al. [24] and Cosenza et al. [14] through calibrating the parameters based on experimental results. It has an ascending curve that represents the bond mechanism of chemical adhesion, a plateau interval with constant maximum bond stress, a linear descending branch and a final horizontal branch with a constant frictional response [27]. The model is adopted by the CEB-FIP Model Code 1990 [28] for traditional steel reinforcements based on a series of parameters (i.e. the peak bond stress  $\tau_{max}$ , the slip corresponding to the peak bond stress  $s_1$  and the parameters  $s_2, s_3, \alpha$  and  $\beta$ ) which depend on the amount of confinement, bond conditions and concrete strength. Fig. 1 and Eqs. (4a)–(4d) describe the bond stress-slip relation curve of this model in which the bond stress is a function of the bond-slip  $s$ .

$$\tau = \tau_{max}(s/s_1)^\alpha \quad \text{for } 0 \leq s \leq s_1 \quad (4a)$$

$$\tau = \tau_{max} \quad \text{for } s_1 < s \leq s_2 \quad (4b)$$

$$\tau = \tau_{max} - (\tau_{max} - \tau_f) \left( \frac{s - s_2}{s_3 - s_2} \right) \quad \text{for } s_2 < s \leq s_3 \quad (4c)$$

$$\tau = \tau_f = \beta\tau_{max} \quad \text{for } s_3 < s \quad (4d)$$

In order to describe the bond-slip behaviour of FRP rebars in concrete by using the BPE Model, the parameters of the BPE Model need to be recalibrated specifically for the FRP rebars. In Rossetti et al.'s study [24], the parameters for GFRP rebars with smooth and rough surfaces and embedded in concrete with different compressive strengths were evaluated. The peak bond stress and the slip corresponding to the peak bond stress were obtained through experimental tests. The parameters  $s_2, s_3, \alpha$  and  $\beta$  were determined through a special identification technique. However, their test results were quite scattered, and the diameter of rebar showed to have no influence on the bond-slip behaviour in their tests.

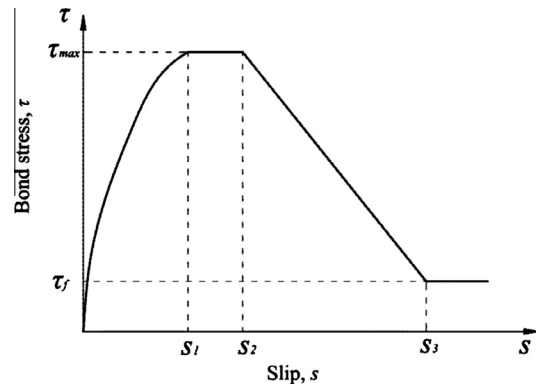


Fig. 1. BPE Model.

Cosenza et al. [14] also carried out experimental studies to determine the parameters of the BPE Model for FRP rebars with various fibre types, rebar surface treatments and confining pressures. The test results for both indented and grain covered rebars were good in terms of bond strength, while those for the spirally wounded rebars were very scattered [14].

### 2.3. BPE Modified Model

The BPE Modified Model (Fig. 2) was proposed by Cosenza et al. [1], and the effect of various rebar surfaces on the bond strength of FRP rebars has been considered in this model. To better describe the bond stress-slip relationship of FRP rebars, the second branch with a constant maximum bond stress in the BPE Model is omitted in the BPE Modified Model. This model also gives a complete bond stress-slip constitutive curve for FRP rebars, and it is more suitable for FRP rebars. However, it should be noted that the effects of different rebar diameter and FRP fibre type have not been taken into account in this model. Eqs. (5a)–(5c) express each part of this curve respectively.

$$\frac{\tau}{\tau_1} = \left(\frac{s}{s_1}\right)^\alpha \quad \text{for } 0 \leq s \leq s_1 \quad (5a)$$

$$\frac{\tau}{\tau_1} = 1 - p\left(\frac{s}{s_1} - 1\right) \quad \text{for } s_1 < s \leq s_3 \quad (5b)$$

$$\tau = \tau_3 \quad \text{for } s_3 < s \quad (5c)$$

### 2.4. CMR Model and Tighiouart et al.'s Model

The CMR Model proposed by Cosenza et al. [14] is a refined model for only the ascending branch of the bond-slip law. This model describes the bond stress-slip constitutive relation of FRP rebars at the serviceability state level, and it is expressed as:

$$\frac{\tau}{\tau_1} = \left[1 - \exp\left(-\frac{s}{s_r}\right)\right]^\varphi \quad (6)$$

where  $s_r$  and  $\varphi$  are parameters based on the curve-fitting of the test data.

FRP rebars with different fibre types and rebar surface treatments were tested in order to determine the parameters in the CMR Model. Some of the test results were very scattered, and the effect of rebar diameter on the bond strength was not investigated.

Tighiouart et al. [5] proposed an alternative model for the ascending branch of the bond stress-slip relationship of FRP rebars. The expression of this curve is given by:

$$\frac{\tau}{\tau_1} = [1 - \exp(4s)]^{0.5} \quad (7)$$

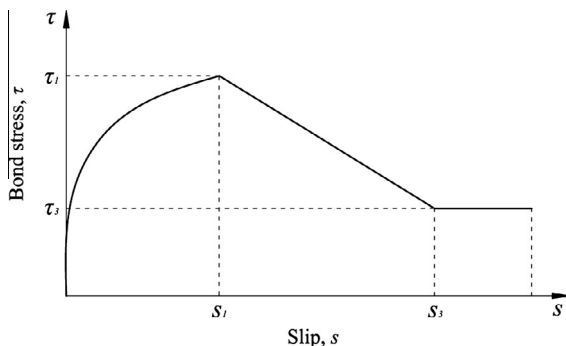


Fig. 2. BPE Modified Model.

It can be seen from Eq. (7) that this model depends on the peak bond stress  $\tau_1$  only. However, according to Tighiouart et al.'s [5] test data, this peak bond stress is affected by some integrated factors, including rebar surface treatment, rebar diameter and embedment length. Therefore, in order to implement this model in the numerical analysis, experimental test has to be conducted based on different cases to determine the peak bond stress  $\tau_1$ . Also, from the mathematic point of view, to have the expression of Eq. (7) make sense,  $1 - e^{4s} \geq 0 \rightarrow e^{4s} \leq 1 \rightarrow s \leq 0$ . Thus, the slip  $s$  in Eq. (7) has to be less than 0. However, it is physically impossible that a slip has a negative value. There must be some mistake in this equation.

It should be mentioned that both CMR Model and Tighiouart et al.'s Model are for the ascending part of the bond-slip relation of FRP only, which may be suitable for modelling of bond at serviceability state level [14] whereas it is insufficient for a complete and accurate numerical analysis of structures till failure.

## 3. Bond stress-slip models of steel rebars in concrete

So far, extensive investigations of the bond-slip behaviour between steel reinforcements and concrete have been reported, and the bond stress-slip constitutive relationships for steel rebars have been derived in a number of studies in addition to the famous BPE Model. In this section, several bond stress-slip models for steel rebars, which may also be suitable for describing the bond-slip behaviour of FRP rebars in concrete, are reviewed and discussed.

### 3.1. Harajli et al.'s Model

An analytical model was proposed by Harajli et al. [16] for describing the local bond stress-slip relationship of steel rebars in plain and fibre reinforced concrete. For pullout bond failure, the shape of the proposed bond stress-slip relation curve is the same as the BPE Model as shown in Fig. 1. The slip  $s_{\max}$  at which the peak bond resistance is mobilised is determined by the clear distance  $c_0$  between the lugs of the steel reinforcing bars by Eq. (8), and it is independent of the concrete strength, confinement and fibre parameters.

$$s_{\max} = 0.2c_0 \quad (8)$$

The four-stage equations for describing the relation between the local bond stress  $\tau$  and slip  $s$  are similar in form to those of the BPE model except for the characteristic parameters. In this model, it is assumed that the influence of rebar diameter on the bond strength is insignificant, and that the model is applicable for rebars with diameter of 8–30 mm. In addition, the effects of other parameters, such as different rebar surfaces, on the bond strength are not included in this model.

### 3.2. Haskett et al.'s Model

A local bond stress-slip model for steel rebars was derived by Haskett et al. [17] from the experimental global load-slip responses obtained from pullout tests. In this model as shown in Fig. 3, the plateau region with a constant peak bond stress in the BPE Model is removed and the frictional component of the bond stress-slip relationship is ignored. The characteristic parameters in the bond stress-slip model were suggested based on the averaged values from experimental test [13], and the effects of different factors, such as rebar diameter, rebar type and rebar surface, on the bond strength have not been taken into account.

The ascending branch of the Haskett et al.'s Model is given by

$$\tau = \tau_{\max}(s/s_1)^{0.4} \quad (9)$$

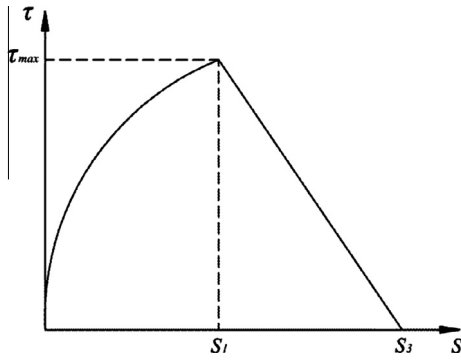


Fig. 3. Haskett et al.'s Model.

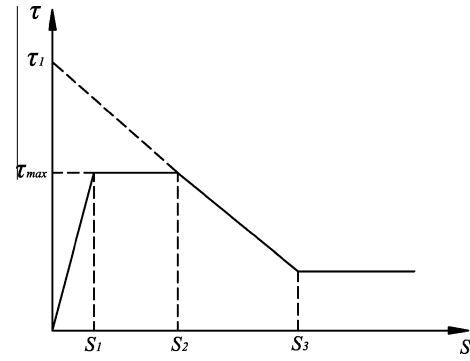


Fig. 4. Yankelevsky's Model.

This equation is the same as the expression suggested by the BPE Model for confined concrete under good bond conditions.

3.3. Soroushian and Choi's Model

Soroushian and Choi [29] investigated the bond-slip behaviour of steel bars in confined concrete, and considered the effect of rebar diameter. It was found that the ultimate local bond stress increased with decreasing bar diameter, whereas the effect of rebar diameter was less significant at larger deformations in the post-peak region. The local bond stress-slip relationship was proposed by Soroushian and Choi [29] based on the experimental results, and its shape is similar to that of the BPE Model (Fig. 1). The ascending curvilinear segment is expressed by

$$\tau = \tau_{max}(s/s_1) \cdot e^{[1-(s/s_1)^\alpha]} \tag{10a}$$

However, the effects of other parameters on the bond strength were not taken into account in this model. Later, Soroushian et al. [30] further investigated the bond-slip behaviour of steel bars in confined concrete with the effects of confinement and concrete compressive strength taken into account. The influence of confinement was found to be insignificant in their study. The peak bond stress  $\tau_{max}$  in the Soroushian and Choi's Model was modified to be determined by both rebar diameter and concrete compressive strength. However, the expression of the ascending curvilinear branch of the Soroushian and Choi's Model reported in Soroushian et al.'s study [30] [Eq. (10b)] is inconsistent with the one given in reference [29] [Eq. (10a)], and the coefficient  $\alpha$  was not given in both studies [29,30].

$$\tau = \tau_{max}(s/s_1) \cdot e^{[1-(s/s_1)^\alpha]/\alpha} \tag{10b}$$

3.4. Yankelevsky's Model

Yankelevsky [31] proposed a local bond stress-slip law which is described by a piecewise linear curve as shown in Fig. 4 and Eqs. (11a)–(11d). However, the characteristic parameters of the model have to be determined by test results, and this makes the model inconvenient to be employed in the finite element analysis directly without doing bond-slip test.

$$\tau = \frac{\tau_{max}}{s_1} \cdot s \text{ for } 0 \leq s \leq s_1 \tag{11a}$$

$$\tau = \tau_{max} \text{ for } s_1 < s \leq s_2 \tag{11b}$$

$$\tau = \tau_1 - \frac{\tau_{max} - \tau_f}{s_3 - s_2} \cdot s \text{ for } s_2 < s \leq s_3 \tag{11c}$$

$$\tau = \tau_f \text{ for } s_3 < s \tag{11d}$$

3.5. Trilinear bond stress-slip model

A simple trilinear bond stress-slip model (Fig. 5) was employed in Kwak and Kim's study [32], in which the parameters were derived from the material properties of specimens from the tests. However, the application of this model is restricted to the cases which do not exhibit significant bond-slip and associated bond damage.

4. Evaluation of bond stress-slip models

Based on the above discussion, the BPE Modified Model seems to be the most suitable bond stress-slip model for FRP rebars in concrete. The BPE Model, the parameters of which were calibrated by Rossetti et al. [24] and Cosenza et al. [14], is also a promising bond stress-slip model to be used in the numerical analysis of FRP-reinforced concrete structures. Although the CMR Model provides only the ascending part of the bond stress-slip constitutive curve, it is of great interest to evaluate it by using it as a substitute for the ascending branch of the BPE Model. In this section, these three bond stress-slip models for FRP rebars are evaluated by building them in a newly-developed finite element model [15] with bond-slip effect for finite element analysis of FRP-reinforced concrete beams. In addition, Harajli et al.'s Model and Haskett et al.'s Model for steel rebars are also implemented in the finite element model to investigate their suitability of being used to model the bond-slip behaviour of FRP rebars in concrete.

4.1. Finite element model

A newly developed composite beam element with the BPE Modified Model representing the bond-slip effect has been demonstrated to be accurate and effective for finite element analysis of

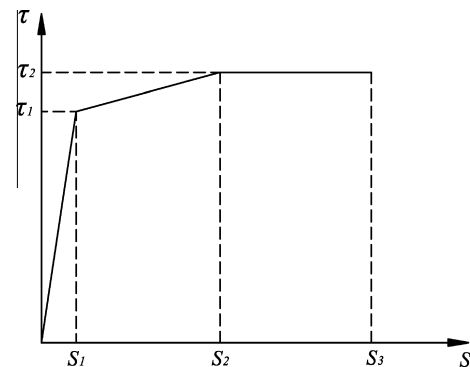


Fig. 5. A trilinear bond stress-slip model.

FRP-reinforced concrete beams [15]. The element is utilised in the current finite element analysis to evaluate the capabilities of various bond stress-slip models. The element is briefly introduced herein for completeness and convenience of referring.

The new composite beam element is shown in Fig. 6. It is a one-dimensional (1D) two-node layered composite beam element with its cross-section composed of a number of concrete layers and reinforcing layers representing the reinforcements. There are four degrees of freedom per node, i.e. transverse displacement  $w$  and rotation  $\theta$  for the concrete beam, and axial displacement  $u$  for each of the reinforcing layers with bond-slip. In order to model the bond-slip effect between the reinforcing bars and surrounding concrete, the nodal degrees of freedom for the reinforcing layers are separated from those for the concrete beam to permit slip, and the reinforcing layer is regarded as a system consisting of two parts: reinforcing bars and the interface between reinforcing bars and the concrete. Thus, a slip is the relative displacement between the reinforcing layer and the concrete.

The element bending strain, shear strain and the strain of the reinforcing layers with bond-slip are expressed as:

$$\varepsilon_b = [B_b]\{q^{(e)}\} \quad \gamma = [B_s]\{q^{(e)}\} \quad \varepsilon_s = [B_{bar}]\{q^{(e)}\} \quad (12)$$

in which

$$[B_b] = \begin{bmatrix} \frac{6\mu_e}{L} \left( \frac{1}{L} - \frac{2x}{L^2} \right) \frac{3\mu_e + 1}{L} - 6\mu_e \frac{x}{L^2} - \frac{6\mu_e}{L} \left( \frac{1}{L} - \frac{2x}{L^2} \right) \\ - \frac{1 - 3\mu_e}{L} - 6\mu_e \frac{x}{L^2} \quad 0 \quad 0 \quad 0 \quad 0 \end{bmatrix} \quad (13a)$$

$$[B_s] = \begin{bmatrix} -\frac{1}{L} + \frac{\mu_e}{L} & \frac{\mu_e}{2} - \frac{1}{2} & \frac{1}{L} - \frac{\mu_e}{L} & -\frac{1}{2} + \frac{\mu_e}{2} & 0 & 0 & 0 & 0 \end{bmatrix} \quad (13b)$$

$$\text{For tensile reinforcement: } [B_{bar}] = \begin{bmatrix} 0 & 0 & 0 & 0 & -\frac{1}{L} & \frac{1}{L} & 0 & 0 \end{bmatrix} \quad (13c)$$

$$\text{For compressive reinforcement: } [B_{bar}] = \begin{bmatrix} 0 & 0 & 0 & 0 & 0 & 0 & -\frac{1}{L} & \frac{1}{L} \end{bmatrix} \quad (13d)$$

where  $[B_b]$  is the curvature-displacement matrix of the concrete beam,  $[B_s]$  the shear strain-displacement matrix of the concrete beam, and  $[B_{bar}]$  the axial strain-displacement matrix of the reinforcing layers with bond-slip,  $L$  is the length of the beam element,  $x$  the coordinate along the beam element, and  $\mu_e$  the coefficient which depends on the element bending stiffness and shear stiffness.

$\{q^{(e)}\}$  is the element nodal displacement vector as follows.

$$\{q^{(e)}\} = \begin{Bmatrix} q_1 \\ q_2 \end{Bmatrix} \quad \text{with} \quad \{q_i\} = \begin{Bmatrix} w_i \\ \theta_i \\ u_{i1} \\ u_{i2} \end{Bmatrix} \quad (i = 1, 2) \quad (14)$$

where  $u_{i1}$  and  $u_{i2}$  are the axial displacements for each of the reinforcing layers with bond-slip.

In order to build the bond stress-slip model into the finite element model, the slip  $s$  is expressed in terms of the bond strain  $\varepsilon_{bond}$  as follows.

$$s = \varepsilon_{bond} L_{GP} \quad (15)$$

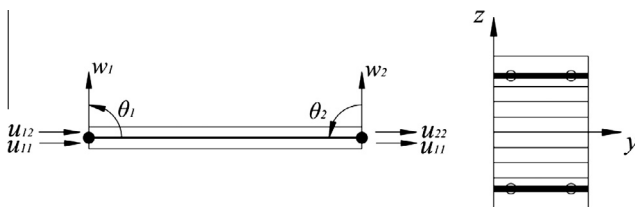


Fig. 6. A 1D two-node composite beam element and its cross-section.

where  $L_{GP}$  is the distance between Gaussian points.

The modulus of the bond  $E_{bond}$  is given by:

$$E_{bond} = \frac{\tau}{s} L_{GP} \quad (16)$$

The finite element equation for this composite beam element is expressed as:

$$[K_T^{(e)}]\{\Delta q^{(e)}\} = \{R^{(e)}\} - \int [B]^T \{\sigma\} dx - \int [B_{bar}]^T \{\sigma_{bar}\} dx \quad (17)$$

where  $\{R^{(e)}\}$  is the element equivalent nodal loadings, and  $[B]$  consisting of  $[B_b]$  and  $[B_s]$  is the strain matrix of the concrete beam.  $\{\sigma\}$  is the internal stress vector of the concrete beam, and  $\{\sigma_{bar}\}$  is the internal stress vector of the reinforcements with bond-slip which is given in the following equation.

$$\{\sigma_{bar}\} = \sum E_{sj} A_{sj} \{\varepsilon_{sj}\} + \sum E_{bond,j} p_j \{\varepsilon_{bond,j}\} \quad (18)$$

where  $E_{sj}$  is the elastic modulus of the  $j$ th reinforcing layer, and  $E_{bond,j}$  the modulus of the bond, which is obtained from the bond stress-slip model.  $A_{sj}$  and  $p_j$  are the area and perimeter of the  $j$ th reinforcing layer respectively.

The total tangential stiffness matrix of the element  $[K_T^{(e)}]$  is partly contributed by the concrete beam and partly by the reinforcements with bond-slip as follows.

$$[K_T^{(e)}] = [K_c^{(e)}] + \sum [K_{sj}^{(e)}] \quad (19)$$

More details about this element can be found from the Ref. [15]. FRP-reinforced concrete beams analysed in this study are discretized using this 1D composite beam element.

#### 4.2. Finite element analysis of a GFRP-reinforced concrete beam

A 2100 mm long GFRP-reinforced concrete beam tested by Qu et al. [33] is modelled using 12 composite beam elements in this study. A four-point bending load is applied to the concrete beam, giving a 600 mm shear span. The beam is reinforced with four 12.7 mm-diameter sand coated GFRP rebars in the bottom area, two steel bars of 10 mm-diameter are placed in the compression zone and 10 mm-diameter steel stirrups are used as shear reinforcement at 100 mm spaces in the shear span. The cubic compressive strength of the concrete is 30.95 MPa, and the tensile strength and elastic modulus of GFRP 782 MPa and 45 GPa respectively.

##### 4.2.1. Finite element analysis of a GFRP-reinforced concrete beam using the BPE Modified Model

The BPE Modified Model is firstly employed in the current finite element analysis to investigate its suitability for FRP rebars. The required parameters in the BPE Modified Model for defining the bond stress-slip relationship of FRP rebars with ribbed, braided, grain-covered and smooth surfaces were calibrated based on the available experimental tests [1], and they are given in Table 1. It should be noted that a grain-covered surface type for FRP reinforcements is selected due to the lack of parameters for FRP rebars with sand-coated surfaces.

Table 1

Parameters for defining bond stress-slip relationship of FRP rebars in the BPE Modified Model [1].

Reinforcement type	Ribbed	Braided	Grain-covered	Smooth
$\alpha$	0.283	0.177	0.067	0.145
$p$	14.88	12.80	3.11	1.87
$s_1$	1.23 mm	2.14 mm	0.13 mm	0.26 mm
$\tau_1$	11.61 MPa	10.20 MPa	12.05 MPa	1.19 MPa
$\tau_3$	7.79 MPa	6.26 MPa	3.17 MPa	0.99 MPa

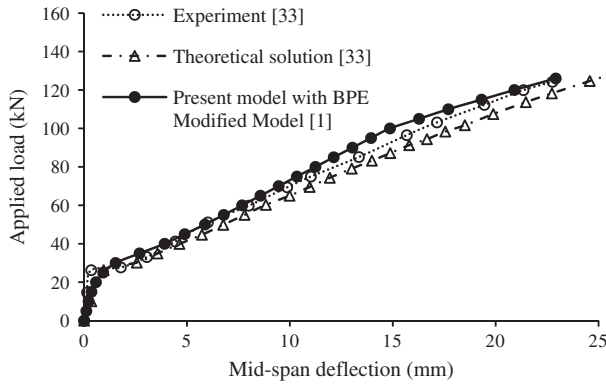


Fig. 7. Load–deflection relationship at mid-span of the GFRP-reinforced concrete beam calculated using the BPE Modified Model.

**Table 2**  
Parameters for defining bond stress-slip relationship of FRP rebars in the BPE Model [24].

Reinforcement type	Rough surface and medium strength concrete	Smooth surface and medium strength concrete	Rough surface and low strength concrete	Rough surface and high strength concrete
$\alpha$	0.25	0.16	0.39	0.12
$\beta$	0.73	0.82	0.72	0.72
$s_1$	0.29 mm	0.42 mm	0.61 mm	0.24 mm
$s_2$	0.76 mm	2.54 mm	1.18 mm	0.37 mm
$s_3$	2.83 mm	4.23 mm	3.74 mm	3.79 mm
$\tau_1$	0.93 MPa	0.5 MPa	0.78 MPa	3.13 MPa

The relationships between the applied load and mid-span deflection obtained from the current model, experimental study [33] and theoretical solution [33] are compared in Fig. 7. It can be seen that the load–deflection curve obtained from the present model matches very well with the test results and theoretical solution attained by Qu et al. [33]. This example illustrates that the BPE Modified Model is appropriate for the current finite element analysis and can model the structural behaviour of the FRP-reinforced concrete beam accurately.

#### 4.2.2. Finite element analysis of a GFRP-reinforced concrete beam using the BPE Model

In this section, the BPE Model is integrated into the finite element model to analyse the GFRP-reinforced concrete beam. The main parameters in the BPE Model based on the experimental tests conducted by Rossetti et al. [24] are given in Table 2. In the current finite element model, reinforcing bars with rough surfaces are used, and the concrete is with low strength.

From the experimental test data, parameters for the BPE Model calibrated by Cosenza et al. [14] are given in Table 3. In this example, the GFRP rebars are sand coated to increase the bond with the concrete, however, the parameters for sand coated braided CFRP rebars are chosen for the current finite element analysis as there is no data available for sand coated GFRP rebars from Cosenza et al.'s [14] test.

The load versus mid-span deflection relationships obtained from numerical analyses with the BPE Models calibrated by Rossetti et al. [24] and Cosenza et al. [14] respectively are compared with the experimental results [33] and Qu et al.'s theoretical solution [33] in Fig. 8. As can be seen, the load versus mid-span deflection relation curve obtained from the finite element model using the bond stress-slip model calibrated by Rossetti et al. [24] devi-

**Table 3**  
Parameters for defining bond stress-slip relationship of FRP rebars in the BPE Model [14].

Reinforcement type	Spirally wounded AFRP	Braided AFRP	Spirally wounded CFRP	Sand coated braided CFRP
$\alpha$	0.36	0.22	0.23	0
$s_1$	4.02 mm	1.30 mm	4.24 mm	0.09 mm
$s_2$	7.68 mm	2.95 mm	6.69 mm	0.82 mm
$\tau_1$	15.66 MPa	11.18 MPa	13.14 MPa	15.50 MPa

ates from the test results immediately after concrete cracks. On the contrary, the load–deflection curve calculated from the numerical model with the bond stress-slip model given by Cosenza et al. [14] is found to have a good agreement with the test data [33] and Qu et al.'s theoretical solution [33]. Therefore, the BPE Model calibrated by Cosenza et al. [14] also appears to be suitable for the finite element analysis of FRP-reinforced concrete beams, whereas the one calibrated by Rossetti et al. [24] seems not to be a good alternative.

#### 4.2.3. Finite element analysis of a GFRP-reinforced concrete beam using the CMR Model

As the CMR Model was proposed as a refined model for the ascending branch of the BPE Model, in order to investigate the appropriateness of the CMR Model in finite element analysis of FRP-reinforced concrete beams, the ascending part of the bond stress-slip curve in the BPE Model is expressed by Eq. (6), and the finite element analysis of the GFRP-reinforced concrete beam is carried out using this model.

The parameters in the CMR Model were calibrated by Cosenza et al. [14] based on their experimental tests and they are shown in Table 4. In the present analysis, parameters for sand coated braided CFRP rebars are selected. The load–deflection relationship at mid-span calculated using the current finite element model is illustrated in Fig. 9 and compared with those obtained from experimental test and theoretical study [33].

It can be found that the predicted load–deflection curve is in good agreement with the test data and the theoretical solution [33]. However, the calculation terminates when the applied load just exceeds 100 kN which is much lower than the experimental test. In this example, the CMR Model performs not as well as the BPE Modified Model and the BPE Model calibrated by Cosenza et al. [14] when being used as bond stress-slip model for FRP rebars.

#### 4.2.4. Finite element analysis of a GFRP-reinforced concrete beam using the Harajli et al.'s Model

The appropriateness of using the bond stress-slip model proposed by Harajli et al. [16] for steel rebars to simulate the bond-slip behaviour of FRP rebars is studied in this section. Eqs. (4a)–(4d) describe the bond stress-slip curve, where  $\alpha = 0.30$ ,  $\tau_{\max} = 2.57\sqrt{f_c}$  MPa,  $\tau_f = 0.35\tau_{\max}$ ,  $s_1 = 0.75s_{\max} = 0.15c_0$ ,  $s_2 = 1.75s_{\max} = 0.35c_0$ ,  $s_3 = c_0$ . In the absence of information about the rebar deformation properties,  $s_1$ ,  $s_2$  and  $s_3$  are taken equal to 1.5 mm, 3.5 mm and 10 mm respectively [34].

The load–deflection relationship at the mid-span of the GFRP-reinforced concrete beam is calculated and compared with the test results [33] and theoretical solution [33] in Fig. 10. As can be seen, the prediction obtained from the current finite element model using Harajli et al.'s [16] bond stress-slip model agrees very well with the experimental results [33] until the applied load exceeds 100 kN. After that, the slope of the calculated load–deflection curve obviously drops and deviation develops. Therefore, the current finite element model using Harajli et al.'s Model could not produce

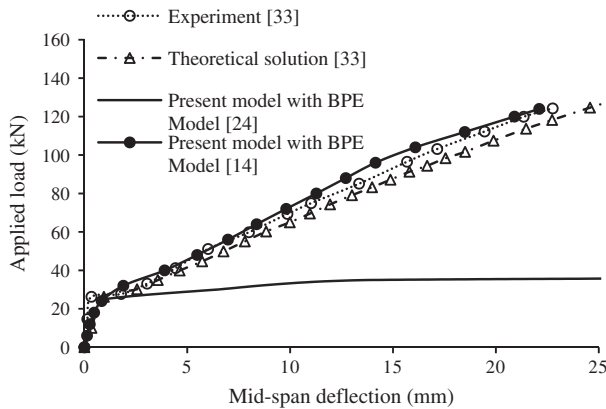


**Fig. 8.** Load–deflection relationships at mid-span of GFRP-reinforced concrete beam calculated using the BPE Model.

**Table 4**  
Parameters for defining bond stress-slip relationship of FRP rebars in CMR Model [14].

Reinforcement type	Spirally wound AFRP	Braided AFRP	Spirally wound CFRP	Sand coated braided CFRP
$\phi$	0.40	0.40	0.26	0
$s_r$	2.78 mm	0.60 mm	3.33 mm	–
$s_2$	7.68 mm	2.95 mm	6.69 mm	0.82 mm
$\tau_1$	15.66 MPa	11.18 MPa	13.14 MPa	15.50 MPa

accurate prediction at the end of loading process. However, it can be found from this example that Harajli et al.’s Model for steel rebars may be possible to be used for FRP rebars provided that its characteristic parameters are modified based on the experimental tests of FRP rebars in concrete.

**4.2.5. Finite element analysis of a GFRP-reinforced concrete beam using the Haskett et al.’s Model**

Haskett et al.’s Model for steel rebars in concrete is lastly employed in this numerical example to investigate its applicability for FRP rebars. The values of characteristic parameters in Haskett et al.’s Model were obtained from test data [13]. It is recommended that  $\tau_{max} = 2.5\sqrt{f'_c}$ ,  $s_1 = 1.5$  mm, and  $s_3 = 15$  mm, where  $f'_c$  is the concrete compressive strength.

The load versus mid-span deflection relationship of the GFRP-reinforced concrete beam obtained from the finite element model using Haskett et al.’s [17] bond stress-slip model is illustrated in Fig. 11. The results from the experimental test [33] and theoretical study [33] are also shown in Fig. 11 for comparison. As can be seen, the discrepancy between the predicted results and the test data [33] starts at the applied load of about 60 kN, and it develops with the increase of load. The phenomenon obtained by using the Haskett et al.’s Model in this example is similar to that using Harajli et al.’s Model, but the performance of the Haskett et al.’s Model is worse than that of the Harajli et al.’s Model.

**4.3. Finite element analysis of a CFRP-reinforced concrete beam**

In order to further evaluate the bond stress-slip models for FRP rebars, a CFRP-reinforced concrete beam tested by Rafi et al. [35] is modelled in this section. The beam has an overall length of 2000 mm and a cross-section of 120 mm × 200 mm. Two 9.5 mm-diameter CFRP bars are placed in the tension zone and two 8 mm-diameter steel bars in the compression area. A 20 mm concrete cover is used all around the beam. The beam is simply supported with a span of 1750 mm under a four-point bending load. The compressive strength of the concrete is 41.71 MPa, the

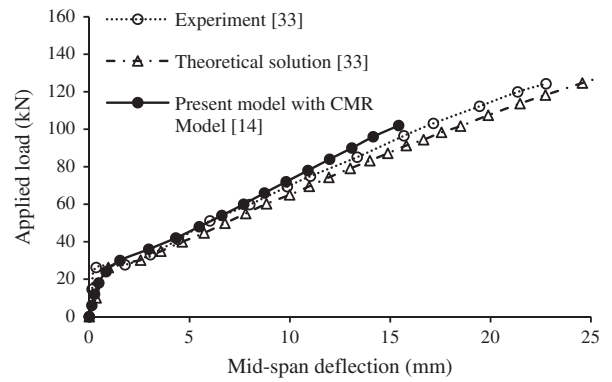


**Fig. 9.** Load–deflection relationship at mid-span of GFRP-reinforced concrete beam calculated using the CMR Model.

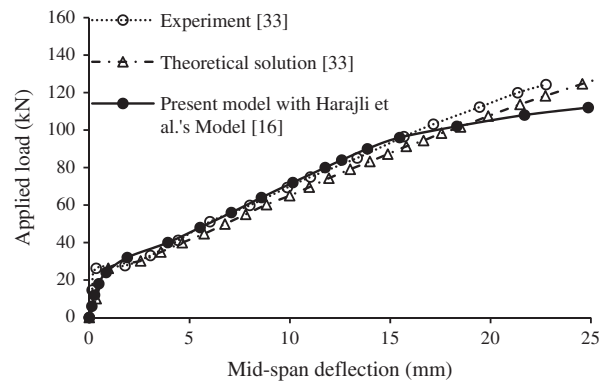


**Fig. 10.** Load–deflection relationship at mid-span of GFRP-reinforced concrete beam calculated using the Harajli et al.’s Model.

ultimate strength and elastic modulus of the CFRP rebars are 1676 MPa and 135.9 GPa respectively, and the yield strength and elastic modulus of the steel rebars are 566 MPa and 194 GPa respectively. The surfaces of the CFRP rebars are textured to increase their bond with the concrete. Eight composite beam elements with 100 concrete layers are used to discretize the CFRP-reinforced concrete beam.

**4.3.1. Finite element analysis of a CFRP-reinforced concrete beam using the BPE Modified Model**

A grain-covered surface for CFRP rebar is assumed in the finite element analysis since there is no data available for a textured FRP rebar surface in the bond stress-slip model. The load–deflection relationships at the mid-span obtained from the test data [35] and the current modelling with the BPE Modified Model are shown in Fig. 12. Very good agreement between the results obtained from the present model and test data [35] is observed. This example further demonstrates the capability of the BPE Modified Model for accurately modelling the bond-slip behaviour of FRP rebars in concrete and its applicability of being used in the finite element analysis.

Moreover, in addition to the global structural behaviour, local strain distribution on the reinforcing bars which can be used to monitor the bond behaviour between the FRP rebars and surrounding concrete is also calculated. Fig. 13 shows the relationships between the applied load and tensile strain distributions on the surface of the FRP rebar at the mid-span and 275 mm from the support in the shear span of the CFRP-reinforced concrete beam obtained from the current finite element model and experimental test [36]. It should be noted that the locations, from which the

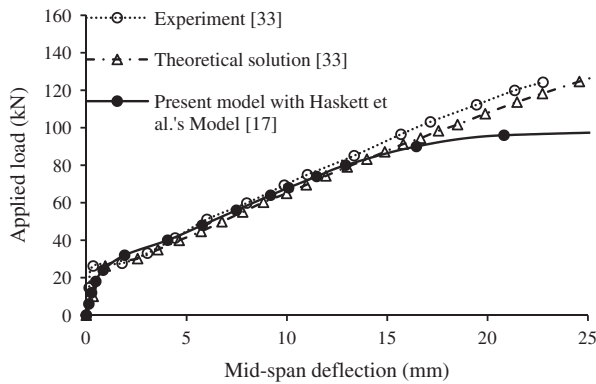


Fig. 11. Load-deflection relationship at mid-span of GFRP-reinforced concrete beam calculated using the Haskett et al.'s Model.

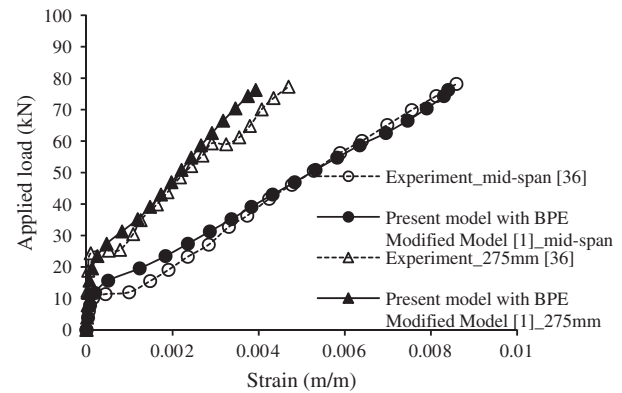


Fig. 13. Rebar strain distributions at mid-span and 275 mm from support of CFRP-reinforced concrete beam calculated using the BPE Modified Model.

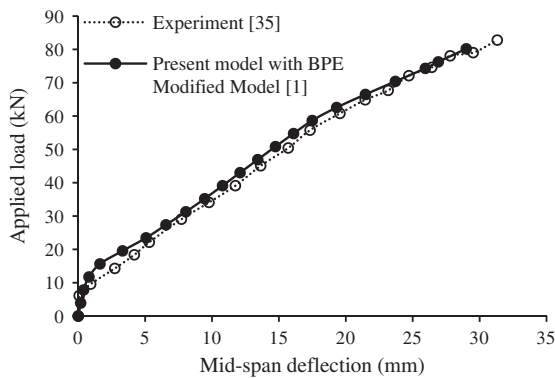


Fig. 12. Load-deflection relationship at mid-span of CFRP-reinforced concrete beam calculated using the BPE Modified Model.

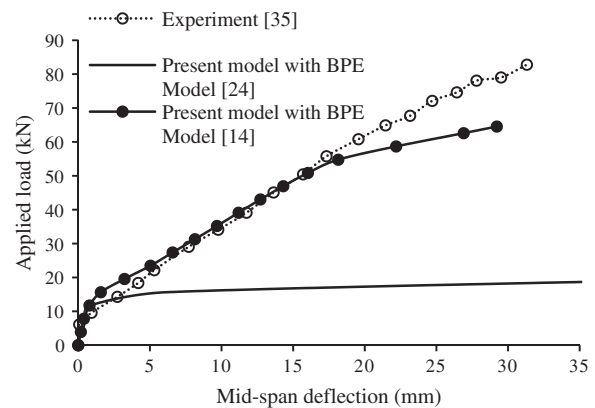


Fig. 14. Load-deflection relationships at mid-span of CFRP-reinforced concrete beam calculated using the BPE Model.

load-strain curves for the current model are obtained, are the Gaussian Points closest to the measured locations. It can be seen that the predicted results from the finite element modelling agree very well with those from the test data [36]. The strain in the CFRP rebars is almost linear up to failure of the beam, which is very similar to its load-deflection relationship. This phenomenon indicates a good transfer of load from the concrete to the reinforcing bars, which agrees well with the findings from the experimental study [36]. The comparison of load-strain curves again validates the appropriateness of using the BPE Modified Model to describe the bond stress-slip relationship of FRP rebars in finite element analysis.

#### 4.3.2. Finite element analysis of a CFRP-reinforced concrete beam using the BPE Model

For finite element analysis using the BPE Model calibrated by Rossetti et al. [24], parameters for reinforcing bars with rough surfaces and embedded in the concrete with low strength are chosen. On the other hand, when employing the BPE Model calibrated by Cosenza et al. [14] in the analysis, parameters for spirally wound CFRP rebars are selected due to the lack of information for CFRP rebars with textured surfaces in Cosenza et al.'s [14] study.

Fig. 14 shows the load-deflection relationships at mid-span of the CFRP-reinforced concrete beam calculated using the finite element model with the BPE Model, as well as the test data from Rafi et al.'s study [35]. The relationships between the applied load and tensile strain distribution on the surface of the CFRP rebar obtained from the finite element model and the test results [36] are illustrated in Fig. 15.

For the finite element model using the BPE Model calibrated by Cosenza et al. [14], it can be seen from Fig. 14 that the load-deflection curve is in good agreement with the test results from the beginning till the applied load at around 50 kN. After that, a deviation develops. In Fig. 15, it can be seen that the load-strain curve calculated at 275 mm from support of the CFRP-reinforced concrete beam agrees well with the test data until the termination of the calculation while the strains obtained at the mid-span of the beam from the finite element model do not agree as well as the one obtained at 275 mm from support with the test results especially when the applied load exceeds 50 kN, which may be attributed to more bond-slip calculated to take place in the mid-span of the beam. The discrepancies found at the end of loading stage in both load-deflection and load-strain curves maybe because more bond-slip is calculated to take place than the experimental test.

As for the finite element model using the BPE Model calibrated by Rossetti et al. [24], both load-deflection relationship and rebar strain distribution obtained from the finite element model do not agree with the test data [36], which can be seen in Figs. 14 and 15. Therefore, the BPE Model calibrated by Rossetti et al. [24] is not suitable to be employed in the current finite element model.

#### 4.3.3. Finite element analysis of a CFRP-reinforced concrete beam using the CMR Model

In the CMR Model, parameters for CFRP rebars with spirally wound surface are selected for the present analysis. The load-deflection relationship at mid-span and the rebar strain distribution at mid-span and 275 mm from support calculated

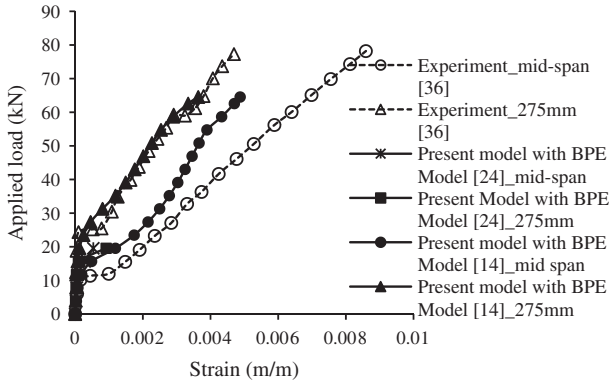


Fig. 15. Rebar strain distributions at mid-span and 275 mm from support of CFRP-reinforced concrete beam calculated using the BPE Model.

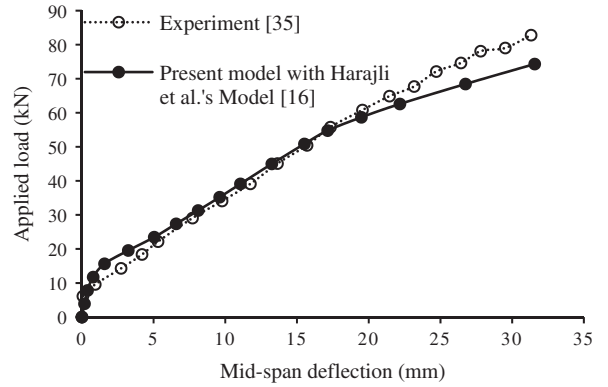


Fig. 18. Load-deflection relationships at mid-span of CFRP-reinforced concrete beam calculated using the Harajli et al.'s Model.

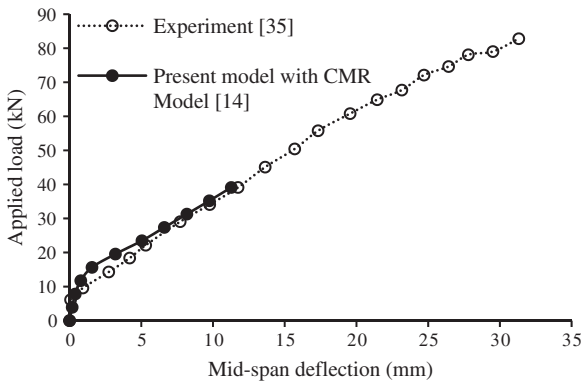


Fig. 16. Load-deflection relationships at mid-span of CFRP-reinforced concrete beam calculated using the CMR Model.

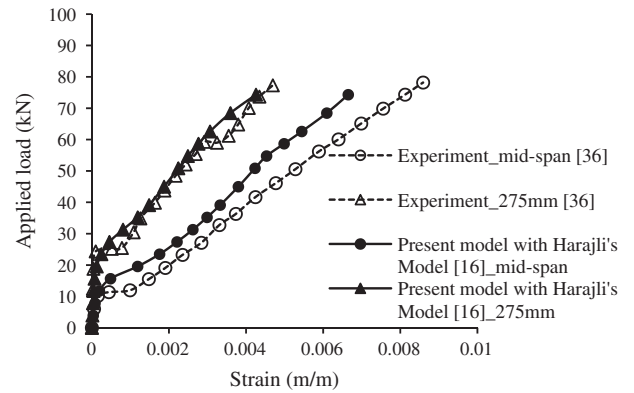


Fig. 19. Rebar strain distributions at mid-span and 275 mm from support of CFRP-reinforced concrete beam calculated using the Harajli et al.'s Model.

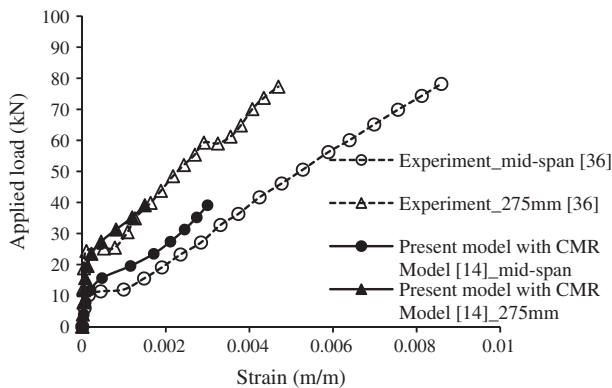


Fig. 17. Rebar strain distributions at mid-span and 275 mm from support of CFRP-reinforced concrete beam calculated using the CMR Model.

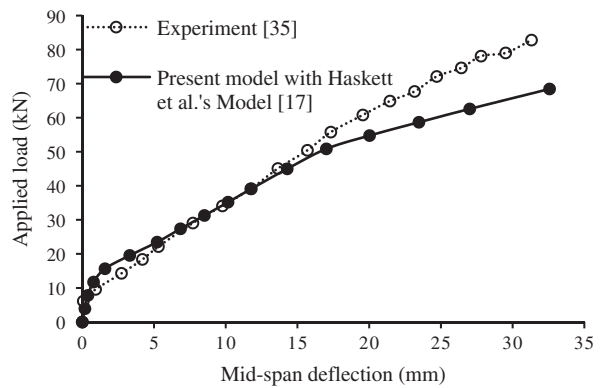


Fig. 20. Load-deflection relationships at mid-span of CFRP-reinforced concrete beam calculated using the Haskett et al.'s Model.

from the finite element model are illustrated in Figs. 16 and 17 respectively, and compared with those obtained from experimental test [35,36].

As can be seen from Figs. 16 and 17, the predicted results agree well with the test data till the applied load at around 40 kN, however, the calculation terminated at the same load level which is much lower than the test result [35,36]. This finding is similar to the one reported in Section 4.2.3, thus it can be concluded that the CMR Model is also not appropriate for being implemented in the finite element analysis.

4.3.4. Finite element analysis of a CFRP-reinforced concrete beam using the Harajli et al.'s Model

In this section, the bond stress-slip model proposed by Harajli et al. [16] for steel rebars is employed in the present finite element model to analyse the CFRP-reinforced concrete beam. The load versus mid-span deflection relationship obtained from the current prediction is compared with that from experimental test [35] and shown in Fig. 18. Fig. 19 shows the relationships between the applied load and the rebar strain distribution at mid-span and at 275 mm from support obtained from both finite element analysis and experimental results [36].

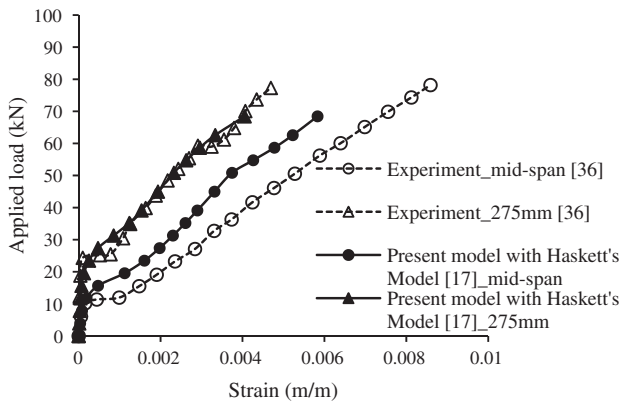


Fig. 21. Rebar strain distributions at mid-span and 275 mm from support of CFRP-reinforced concrete beam calculated using the Haskett et al.'s Model.

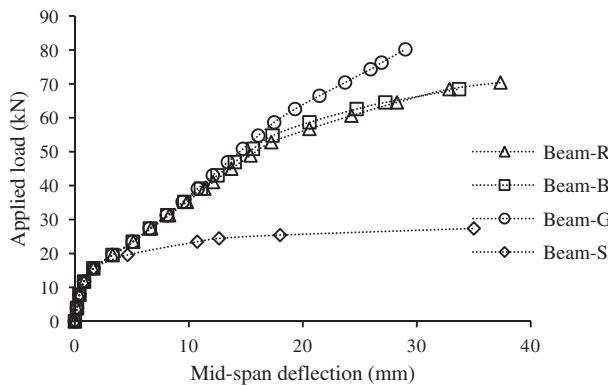


Fig. 22. Load-deflection relationships at mid-spans of CFRP-reinforced concrete beams with different rebar surfaces.

It can be seen from Fig. 18 that the predicted results obtained from the current finite element model are in excellent agreement with the test data [35] until the applied load at around 60 kN. The discrepancy between the calculated results and test results [35] is found after that. This phenomenon is similar to that observed in Section 4.2.4. In Fig. 19, there is a very good agreement between the numerical results and test data [36] for the rebar strain at 275 mm from the support, whereas a small amount of discrepancy is found between the two studies at mid-span of the beam, and this discrepancy increases at the end of loading stage. This may be attributed to more bond-slip is predicted to take place in the mid-span, and the capacity of the Harajli et al.'s Model is limited. Based on the above two examples, the Harajli et al.'s Model is found to have potential to be used for modelling of bond-slip behaviour of FRP rebars in concrete, but more efforts are needed to improve this model.

#### 4.3.5. Finite element analysis of a CFRP-reinforced concrete beam using the Haskett et al.'s Model

Haskett et al.'s Model is applied in this section for analysis of the CFRP-reinforced concrete beam. The load-deflection relationship and the load-rebar strain relationships are calculated and shown in Fig. 20 and Fig. 21 respectively. The results from the experimental test [35,36] are also given for comparison.

As can be seen from Fig. 20 that the discrepancy between the predicted load-deflection relation curve and the test data [35] can be found at the applied load of about 45 kN, and it increases with the increase in load. And the predicted maximum bearing load is much lower than the test result [35]. Fig. 21 also shows

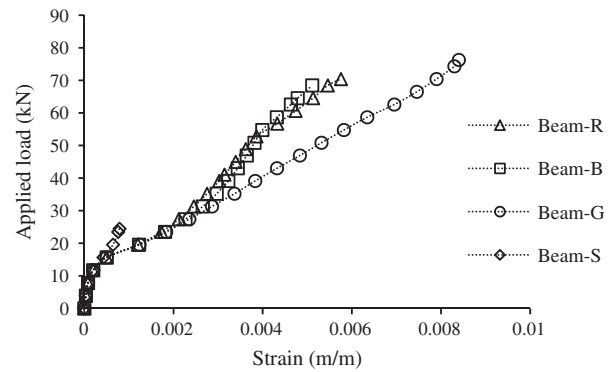


Fig. 23. Rebar strain distributions at mid-spans of CFRP-reinforced concrete beams with different rebar surfaces.

the imprecise predictions given by the model using Haskett et al.'s [17] bond stress-slip model. This example further demonstrates that the performance of Haskett et al.'s Model is worse than that of Harajli et al.'s Model when being used to model the bond-slip behaviour of FRP rebars in concrete.

## 5. Parametric study

Based on the numerical evaluation in Section 4, the BPE Modified Model is demonstrated to be the most appropriate bond stress-slip model that currently available for numerical analysis of FRP-reinforced concrete structures, though it has only considered the effect of different rebar surfaces on the bond strength. In order to show the sensitivity of structural behaviour of FRP-reinforced concrete structures to the rebar surface treatment, parametric study is carried out in this section by using four different types of rebar surface. The CFRP-reinforced concrete beam in Section 4.3 is used as the basic model. Four beams, named Beam-R, Beam-B, Beam-G and Beam-S, for CFRP rebars with ribbed, braided, grain-covered and smooth surfaces respectively are analysed. All beams have the same dimensions and loading systems. The load-deflection relationships at mid-span obtained from the current finite element model with the BPE Modified Model are shown in Fig. 22.

It can be seen that CFRP-reinforced concrete beams with different rebar surfaces differ greatly in terms of their flexural behaviour under loading. The concrete beam reinforced with grain-covered CFRP rebars shows the best structural performance and can sustain the most loads with the least deflection whereas the beam reinforced with smooth CFRP rebars performs the worst, which can only bear a small amount of load and fails earlier than the others. The load-deflection curve for Beam-G is almost linear before concrete cracking and there is only a very minor change in the slope of the curve at the end of the loading stage which indicates that a small amount of slippage may take place. Therefore, it can be concluded that a good bond exists between the CFRP bars with grain-covered surfaces and the surrounding concrete.

The load-deflection curves for Beam-R and Beam-B are very close to each other, with both showing linear behaviour at the early stage of loading and being both close to that of Beam-G. Good bonds in both Beam-R and Beam-B are observed until a load of about 53 kN when obvious changes in the slopes of their load-deflection curves are found. This means that the stiffness of each structure decreases suddenly at that point, which may be caused by slip between the reinforcing bars and the surrounding concrete, thereby causing failure in the force transfer across the interface between the two components.

For FRP rebars with smooth surfaces, due to the lack of bonding action between rebar surfaces and the concrete, large slip may take

place as soon as the concrete cracks, even at the initial loading stage. Thus, a sharp increase in deflection occurs which may cause the early failure of the whole structure.

The strain distributions of the rebars at the mid-spans of all these four beams are also computed using the current finite element model and shown in Fig. 23. They also indicate a good bond condition in CFRP rebars with grain-covered surfaces while noticeable slips occur in both Beam-R and Beam-B, and Beam-S fails at a very early loading stage.

## 6. Conclusions

In order to generate more accurate results for structural analysis of FRP-reinforced concrete structures, it is of great importance to include bond-slip effect of FRP rebars in the finite element model. However, very few mature bond stress-slip models for FRP rebars have been reported so far. In this paper, several currently available bond stress-slip models for steel and FRP rebars are reviewed, and three most promising models for FRP rebars and two models for steel rebars are evaluated by building them into a newly-developed finite element model for analysis of FRP-reinforced concrete beams. Although the Malvar's Model gives a complete description of the bond stress-slip relation curve of FRP rebars, it is assessed to be less comprehensive and less reliable. The Tighiouart et al.'s Model describes the ascending part of the bond stress-slip curve, but it is found to have mistake in its expression. By comparing the numerical results, the BPE Model calibrated by Rossetti et al. [24] has found to be not applicable to be implemented in numerical analysis. The BPE Model calibrated by Cosenza et al. [14] can produce much better results than the one calibrated by Rossetti et al. [24] when being used to model the bond-slip behaviour of FRP rebars in numerical model, however, the results are not consistent for different cases. In addition, good predictions can only be generated at the beginning of loading by using the CMR Model, and the predicted bearing capacity is much lower than the test data. The predictions given by the finite element analysis using bond stress-slip models for steel rebars, i.e. Harajli et al.'s Model and Haskett et al.'s Model, are not accurate enough, and the discrepancies develop with the increase in load. From this study, the BPE Modified Model is demonstrated to be the best bond stress-slip model for FRP rebars among the others. In the numerical analyses of GFRP and CFRP-reinforced concrete beams, the finite element model with the BPE Modified Model gives very good predictions for both the global structural behaviour of concrete beams and the local strain on the reinforcing bars, and the calculated results are more accurate and consistent than the others. However, the BPE Modified Model is not without its deficiencies, such as the negligence of the effects of rebar diameter and fibre type in the model, therefore further work on the bond strength and bond stress-slip constitutive relationship of FRP rebars is still in demand, especially the effects of various factors on the bond behaviour should be taken into account.

Parametric study is also carried out based on the BPE Modified Model to investigate the effect of rebar surface on the structural behaviour of FRP-reinforced concrete structures. It is found that the type of rebar surface has a significant influence on bond strength and structural behaviour. The grain-covered surface provides the best bond between the FRP rebars and concrete, the smooth surface the worst, and FRP rebars with ribbed and braided surfaces perform similarly.

## References

- Cosenza E, Manfredi G, Realonzo R. Behavior and modeling of bond of FRP rebars to concrete. *J Compos Constr* 1997;1(2):40–51.
- Achillides Z, Pilakoutas K. Bond behavior of fiber reinforced polymer bars under direct pullout conditions. *J Compos Constr* 2004;8(2):173–81.
- Aiello MA, Leone M, Pecce M. Bond performances of FRP rebars-reinforced concrete. *J Mater Civ Eng* 2007;19(3):205–13.
- Okelo R, Yuan RL. Bond strength of fiber reinforced polymer rebars in normal strength concrete. *J Compos Constr* 2005;9(3):203–13.
- Tighiouart B, Benmokrane B, Gao D. Investigation of bond in concrete member with fibre reinforced polymer (FRP) bars. *Constr Build Mater* 1998;12(8):453–62.
- Malvar LJ, Cox JV, Cochran KB. Bond between carbon fiber reinforced polymer bars and concrete. I: experimental study. *J Compos Constr* 2001;7(2):154–63.
- Rafi MM, Nadjai A, Ali F. Analytical modeling of concrete beams reinforced with carbon FRP bars. *J Compos Mater* 2007;41(22):2675–90.
- Nour A, Massicotte B, Yildiz E, Koval V. Finite element modeling of concrete structures reinforced with internal and external fibre-reinforced polymers. *Can J Civ Eng* 2007;34(3):340–54.
- Gomes HM, Awruch AM. Some aspects on three-dimensional numerical modelling of reinforced concrete structures using the finite element method. *Adv Eng Softw* 2001;32(4):257–77.
- Ferreira AJM, Camanho PP, Marques AT, Fernandes AA. Modelling of concrete beams reinforced with FRP re-bars. *Compos Struct* 2001;53(1):107–16.
- Ferreira AJM, Ribeiro MCS, Marques AT. Analysis of hybrid beams composed of GFRP profiles and polymer concrete. *Int J Mech Mater Des* 2004;1(2):143–55.
- Rafi MM, Nadjai A, Ali F. Finite element modeling of carbon fiber-reinforced polymer reinforced concrete beams under elevated temperatures. *ACI Struct J* 2008;105(6):701–10.
- Eligehausen R, Popov EP, Bertero VV. Local bond stress-slip relationships of deformed bars under generalized excitations: experimental results and analytical model. Berkeley: Earthquake Engineering Research Center, University of California; 1983.
- Cosenza E, Manfredi G, Realonzo R. Analytical modelling of bond between FRP reinforcing bars and concrete. In: Taerwe L, editor. *Nonmetallic (FRP) reinforcement for concrete structures*. London: E & FN Spon; 1995. p. 164–71.
- Lin X, Zhang YX. A novel composite beam element with bond-slip for nonlinear finite element analyses of steel/FRP-reinforced concrete beams. *J Struct Eng* 2013. [http://dx.doi.org/10.1061/\(ASCE\)ST.1943-541X.0000829](http://dx.doi.org/10.1061/(ASCE)ST.1943-541X.0000829).
- Harajli MH, Hout M, Jalkh W. Local bond stress-slip behavior of reinforcing bars embedded in plain and fiber concrete. *ACI Mater J* 1995;92(4):343–53.
- Haskett M, Oehlers DJ, Ali MSM. Local and global bond characteristics of steel reinforcing bars. *Eng Struct* 2008;30(2):376–83.
- Malvar LJ. Bond stress-slip characteristics of FRP rebars. California: Naval Facilities Engineering Service Center; 1994.
- Monti G, Spacone E. Reinforced concrete fiber beam element with bond-slip. *J Struct Eng* 2000;126(6):654–61.
- Salari MR, Spacone E. Finite element formulations of one-dimensional elements with bond-slip. *Eng Struct* 2001;23(7):815–26.
- Oliveira RS, Ramalho MA, Corrêa MRS. A layered finite element for reinforced concrete beams with bond-slip effects. *Cem Concr Compos* 2008;30(3):245–52.
- Jendele L, Cervenka J. Finite element modelling of reinforcement with bond. *Comput Struct* 2006;84(28):1780–91.
- Lundgren K, Kettil P, Hanjari KZ, Schlune H, Roman ASS. Analytical model for the bond-slip behaviour of corroded ribbed reinforcement. *Struct Infrastruct Eng* 2012;8(2):157–69.
- Rossetti VA, Galeota D, Giammatteo MM. Local bond stress-slip relationships of glass fibre reinforced plastic bars embedded in concrete. *Mater Struct* 1995;28(6):340–4.
- Pecce M, Manfredi G, Realonzo R, Cosenza E. Experimental and analytical evaluation of bond properties of GFRP bars. *J Mater Civ Eng* 2001;13(4):282–90.
- Focacci F, Nanni A, Bakis CE. Local bond-slip relationship for FRP reinforcement in concrete. *J Compos for Constr* 2000;4(1):24–31.
- Gravina RJ, Smith ST. Flexural behaviour of indeterminate concrete beams reinforced with FRP bars. *Eng Struct* 2008;30(9):2370–80.
- Comite Euro-International du Beton. CEB-FIP model code 1990. Lausanne: Thomas Telford Services Ltd., 1993.
- Soroushian P, Choi K-B. Local bond of deformed bars with different diameters in confined concrete. *ACI Struct J* 1989;86(2):217–22.
- Soroushian P, Choi K-B, Park G-H, Aslani F. Bond of deformed bars to concrete: effects of confinement and strength of concrete. *ACI Mater J* 1991;88(3):227–32.
- Yankelevsky DZ. New finite element for bond-slip analysis. *J Struct Eng* 1985;111(7):1533–42.
- Kwak H-G, Kim S-P. Bond-slip behavior under monotonic uniaxial loads. *Eng Struct* 2001;23(3):298–309.
- Qu W, Zhang X, Huang H. Flexural behavior of concrete beams reinforced with hybrid (GFRP and steel) bars. *J Compos Constr* 2009;13(5):350–9.
- Harajli M, Hamad B, Karam K. Bond-slip response of reinforcing bars embedded in plain and fiber concrete. *J Mater Civ Eng* 2002;14(6):503–11.
- Rafi MM, Nadjai A, Ali F, Talamona D. Aspects of behaviour of CFRP reinforced concrete beams in bending. *Constr Build Mater* 2008;22(3):277–85.
- Rafi MM, Nadjai A, Ali F. Experimental testing of concrete beams reinforced with carbon FRP bars. *J Compos Mater* 2007;41(22):2657–73.